England. It is in the form of flakes which are 2 μm thick and 20 to 50 μm in diameter.

[6]M. I. Aalto, H. K. Collan, R. G. Gylling, and K. O. Nores, Rev. Sci. Instrum. 44, 1075 (1973).

[7]D. D. Osheroff, W. J. Gully, R. C. Richardson, and D. M. Lee, Phys. Rev. Lett. 29, 920 (1972).

[8]W. P. Halperin, C. N. Archie, F. B. Rasmussen, and R. C. Richardson, to be published; W. P. Halperin, R. A. Buhrman, D. M. Lee, and R. C. Richardson, Phys. Lett. 45A, 233 (1973).

Superfluid Mass of Liquid Helium Three*

A. W. Yanof and J. D. Reppy
Laboratory of Atomic and Solid State Physics and The Materials Science Center, Cornell University, Ithaca, New York 14850
(Received 8 July 1974)

Fourth sound has been generated and detected in the superfluid phases of liquid ^{3}He by means of a new technique.

The discovery of transitions to new phases of liquid ^{3}He in the millikelvin temperature range by Osheroff *et al.*[1] revitalized old speculations about the possible superfluidity of liquid ^{3}He. A convincing demonstration of superfluidity has been provided by measurements of fourth-sound modes in liquid ^{3}He by Kojima, Paulson, and Wheatley,[2] and more recently by our group.[3]

Kojima, Paulson, and Wheatley[2] have employed the technique developed by Shapiro and Rudnick[4] to obtain the fourth-sound velocity. The porous medium used is a compressed powder of cerium magnesium nitrate (CMN) which also serves as a refrigerant and thermometer. Drawing a reasonable analogy to fourth sound in ^{4}He, Kojima, Paulson, and Wheatley[2] interpret their results in terms of simple two-fluid hydrodynamics and obtain the superfluid fraction ρ_s/ρ from the expression[4]

$$\rho_s/\rho = n^2(c_4/c_1)^2, \quad (1)$$

where c_4 is the measured velocity of fourth sound and c_1 is the velocity of ordinary sound in bulk liquid. The factor n^2 is a correction term which arises from the complex geometry of the porous medium through which the fourth sound must propagate.

In the work reported here, we employ the method developed by Hall, Kiewiet, and Reppy.[5] Fourth sound is generated by oscillating the entire sample chamber. The liquid properties are then deduced from the response of the sample chamber to a known applied force, and the inertial mass of the oscillating superfluid is obtained directly. This independent measurement can be compared to the value of superfluid density obtained from Eq. (1), thus giving a partial test of the validity of the simple two-fluid model for ^{3}He.

The apparatus is shown in Fig. 1. A cylindrical sample chamber, packed with CMN powder, is suspended elastically by an epoxy rod inside a massive epoxy incasement. An electrode mounted in the incasement drives the cell electrostatically along the cylinder axis. The resulting cell displacement X is sensed electrostatically and monitored by two lock-in amplifiers in quadrature.

Figure 2(a) shows the frequency response with the cell filled with liquid ^{4}He at a temperature of 0.5 K. At 0.7 kHz a suspension resonance is seen. Here the cell oscillates along its axis at

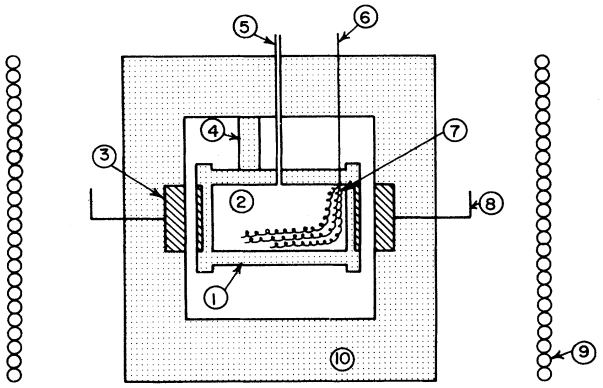

FIG. 1. Schematic diagram of fourth-sound apparatus. 1, Epoxy sample chamber; 2, packed powder (see Ref. 4); 3, metal electrode for driving cavity electrostatically; 4, epoxy suspension rod; 5, fill capillary; 6, high-purity copper wire to heat switch and mixing chamber; 7, wire brush (40 cm^2 surface area); 8, electrode for detecting cavity motion; 9, susceptibility coils and solenoid for magnetic cooling; 10, massive epoxy incasement.

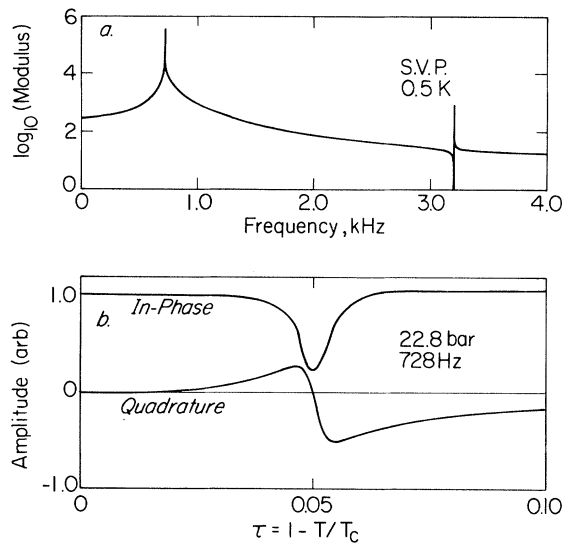

FIG. 2. Response of fourth-sound apparatus. (a) Frequency response of cell filled with ^{4}He. (b) Both quadratures of cell displacement at the suspension-resonance frequency as a function of reduced temperature τ, for the ^{3}He-filled cavity. The fundamental longitudinal fourth-sound resonance occurs at approximately $\tau = 0.05$.

the natural frequency determined by its mass and the stiffness of the suspension rod. The higher-frequency resonance is the fundamental fourth-sound standing wave at 3.2 kHz. When the resonant frequencies of the suspension and the fourth-sound modes are widely separated they may be considered independently. However, in our ^{3}He measurements a fourth-sound frequency crosses the suspension resonance; at crossing, the suspension system becomes a sensitive detector of the fourth-sound mode.

At the beginning of a run, the drive frequency is fixed at the value which maximizes the suspension-resonance amplitude while the ^{3}He is still in the normal phase. The cell is cooled to the lowest possible temperature by demagnetizing the CMN, and the displacement of the cell, $X(\omega, t, \tau)$, is monitored during the subsequent warm-up. Figure 2(b) shows the two quadrature components of the amplitude of the cavity displacement as a function of reduced temperature τ.

The superfluid mass m_s and the fourth-sound quality factor Q_4 are obtained from an analysis of the response curves shown in Fig. 2(b). The displacement X of the cell is determined by the force equation

$$F_0 e^{i\omega t} - KX - D\dot{X} - m_s\ddot{Y} = (M + m - m_s)\ddot{X}, \qquad (2)$$

where $F_0 e^{i\omega t}$ is the drive force along the cylinder axis; K and D are the spring and damping constants of the cell support; M and m are the mass of the cell and the total mass of the fluid within the cell. The term $m_s\ddot{Y}$ is the reaction force due to the acceleration of the center of mass Y of the superfluid within the cell.

To obtain the motion of the fluid we require a slight generalization of the usual fourth-sound wave equation which will allow for the acceleration of the porous medium as well as that of the superfluid. Let x be the coordinate in the rest frame along the axis of motion of the cell. We wish to develop a wave equation for the average superfluid displacement ξ_s in the x direction. The averaging is understood to take place over a volume of fluid large compared to the characteristic dimensions of the porous medium yet small in comparison with the fourth-sound wavelength.

The actual superfluid velocity $\vec{v}_s$ can be expressed as $\vec{v}_s = \dot{\vec{X}} + \nabla\varphi$, where $\dot{\vec{X}}$ is the velocity of the porous medium or cell and φ is a potential function which satisfies the boundary conditions imposed by the complex geometry of the porous medium. We shall define ϵ_1 and ϵ_2 as the volume averages, in the sense mentioned above, of the quantities $\partial\varphi/\partial x$ and $|\nabla\varphi|^2$, respectively. Then the average superfluid velocity in the x direction may be expressed as $\dot{\xi}_s = \dot{X} + \epsilon_1$.

The average kinetic energy density is given by

$$T = \tfrac{1}{2}\rho_s[\dot{\xi}_s^{\,2} + (\epsilon_2\epsilon_1^{-2} - 1)(\dot{\xi}_s - \dot{X})^2].$$

We can now write a Lagrangian density for the fluid as $\mathcal{L} = T - (\rho_s c^2/\rho)(\partial\xi_s/\partial x)^2$. The constant c in the potential energy term will be equal to c_1, the bulk sound velocity, in the absence of any thermal terms. The fourth-sound equation obtained from the Lagrangian density is

$$\frac{\partial^2\xi_s}{\partial t^2} - \frac{\rho_s\epsilon_1^{\,2}c^2}{\rho\epsilon_2}\frac{\partial^2\xi_s}{\partial x^2} - \left(1 - \frac{\epsilon_1^{\,2}}{\epsilon_2}\right)\ddot{X} = 0. \qquad (3)$$

We define $n^2 \equiv \epsilon_2/\epsilon_1^{\,2}$ in making the connection with the fourth-sound velocity expression, Eq. (1), introduced by Shapiro and Rudnick.[4] In Eq. (3) the factor $1 - \epsilon_1^{\,2}/\epsilon_2$ represents that fraction of the superfluid which adds an induced hydrodynamic mass to the porous medium during acceleration.[6] A damping term, $\eta\rho_s^{-1}(\dot{X} - \dot{\xi}_s)$, is added to Eq. (3) to allow for possible attenuation.

Finally, Eqs. (2) and (3), augmented by the

damping term, determine the motion of the cell:

$$X = F_0 e^{i\omega t}\{K - (M+m)\omega^2 - i\omega D + (m_s/n^2)[1 - (2/kL)\tan(\tfrac{1}{2}kL)](\omega/c_4 k)^2\}^{-1}, \quad (4)$$

where L is the length of the cavity and k is a complex quantity given by $k = \omega c_4^{-1}(1 + iQ_4^{-1})^{1/2}$, where $Q_4 = \omega\rho_s\eta^{-1}$.

We fit Eq. (4) to the observed response curves such as shown in Fig. 2(b) to determine the values of m_s/n^2 and Q_4 for the temperature at which the drive and fourth-sound fundamental-mode frequencies coincide. The superfluid fraction, $\rho_s/\rho = m_s/m$, is then obtained by using a value of n^2 taken from ^{4}He measurements. In Fig. 3 agreement is shown between a value of ρ_s/ρ, open circle, obtained by this method and values generated from the temperature dependence of c_4 through the use of Eq. (1). This indicates that thermal terms are not important in the present experiment.

The temperature dependence of c_4 was determined from observation of the passage of a number of different fourth-sound modes through the suspension-resonance frequency. The range of temperature coverage was extended by using a number of different suspension frequencies ranging from 0.7 to 1.8 kHz.

These observations have been made at a number of pressures. For a given reduced temperature we see only a 10% increase in superfluid density as the pressure is increased from 15.9 to 27 bars. The data at these two pressures are indicated in Fig. 3 by the dashed lines. The 32-bar curve published by Kojima, Paulson, and Wheatley[2] lies only a few percent higher than our 27-bar curve. This agreement is most interesting in view of the differences in the packing fraction and geometric factor n^2 for the two fourth-sound cells.[7]

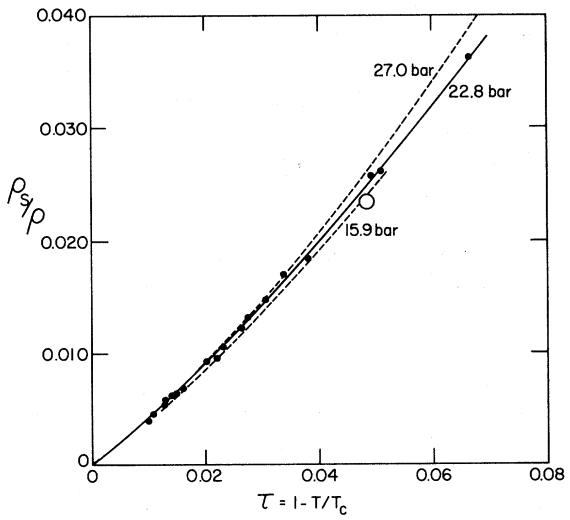

FIG. 3. Superfluid fraction in ^{3}He as a function of reduced temperature. Data points shown are measurements at 22.8 bar.

The fourth-sound quality factor Q_4 is also obtained from the fitting of Eq. (4) to the observed response curves. We find that the value of Q_4 for a given mode shows no systematic variation with temperature. A temperature-independent value for Q_4 would imply that the damping coefficient η approaches zero at the transition approximately as $\tau^{3/2}$. However, there is some mode dependence of Q_4; thus for the fundamental mode we find $Q_4 = 65$ at $\tau = 0.05$ while $Q_4 = 32$ for the second harmonic.

Much higher values of Q_4 are obtained at low temperatures with ^{4}He in the cell. For instance, at 0.2 K, a value of $Q_4 = 2\times10^4$ is observed for the fundamental mode. At higher temperatures the value of Q_4 decreases ($Q_4 = 160$ at 1.5 K). Under the assumption that fourth-sound attenuation is due to imperfect damping of the normal component, one obtains an estimate of the pore size from the observed temperature dependence of Q_4 and the known values of viscosity and superfluid density.[8] Inverting this analysis, and using a viscosity value from Alvesalo *et al.*[9] and an average pore size estimate of 2 μm from the ^{4}He data, we would expect a value of $Q_4 = 500$ for the ^{3}He fundamental mode at $\tau = 0.05$. In contrast the measured value is 65 at this temperature. Thus the mechanism of normal-fluid slippage seems inadequate to account fully for the Q values observed for fourth-sound modes in ^{3}He. Note that the maximum superfluid velocity at the resonance shown in Fig. 2(b) is 1 mm sec^{-1}.

The authors thank R. C. Richardson for his help in many phases of this work. We express our gratitude to the other members of the Cornell University low-temperature group and the Laboratory of Atomic and Solid State Physics theory group for their assistance. One of us (J.D.R.) wishes to thank the Guggenheim Foundation for Fellowship support and Professor H. E. Hass for many stimulating discussions.

*Work supported in part by the National Science Foundation through Grants No. GH-37658, No. GH-35692, and No. GH-38785, and also under Grant No.

GH-33637 through the Cornell Materials Science Center, Report No. 2246.

[1]D. D. Osheroff, W. J. Gully, R. C. Richardson, and D. M. Lee, Phys. Rev. Lett. 29, 920 (1972).

[2]H. Kojima, D. N. Paulson, and J. C. Wheatley, Phys. Rev. Lett. 32, 141 (1974).

[3]A. W. Yanof, E. Smith, D. M. Lee, R. C. Richardson, and J. D. Reppy, Bull. Amer. Phys. Soc. 19, 435 (1974).

[4]K. A. Shapiro and I. Rudnick, Phys. Rev. 137, A1383 (1965).

[5]H. E. Hall, C. Kiewiet, and J. D. Reppy, to be published.

[6]Equation (2) may be applied to the discussion of persistent currents in a porous medium given by J. B. Mehl and W. Zimmerman, Jr., Phys. Rev. 167, 214 (1968). The quantity χ defined by these authors is equal to the coefficient $1-\epsilon_1^2/\epsilon_2$.

[7,4]He measurements give $n^2=2.53$ in our cell, 4.84 in the cell of Ref. 2. In their cell, CMN grains passed through a 35-μm sieve were packed to 80% packing fraction. In our cell 4.15 g of CMN of 50-μm average particle size was combined with 0.42 g of 1-μm Linde aluminum oxide and hand packed into the 2.96 cm^3 volume of the sample chamber. This resulted in an open volume of 0.83 cm^3, a packing fraction of 72%.

[8]D. G. Sanikidze, I. N. Adamenko, and M. I. Kaganov, Zh. Eksp. Teor. Fiz. 52, 584 (1967) [Sov. Phys. JETP 25, 383 (1967)]; I. N. Adamenko and M. I. Kaganov, Zh. Eksp. Teor. Fiz. 53, 615 (1967) [Sov. Phys. JETP 26, 394 (1968)].

[9]T. A. Alvesalo, Yu. D. Anufriyev, H. K. Collan, O. V. Lounasmaa, and P. Wennerström, Phys. Rev. Lett. 30, 962 (1973).

Time-Resolved Laser-Plasma Backscatter Studies*

B. H. Ripin, J. M. McMahon, E. A. McLean, W. M. Manheimer, and J. A. Stamper
Naval Research Laboratory, Washington, D. C. 20375
(Received 20 May 1974)

Time-resolved and time-integrated measurements of the energy, spectra, and other characteristics of the backscattered laser radiation from a laser-produced plasma are presented. Theoretical comparison shows that most of these measurements are consistent with the stimulated-Brillouin-backscattering instability.

The mechanisms responsible for absorption and reflection of laser energy in plasma are of prime importance and concern in laser fusion. The reflection of laser energy by the irradiated target represents a potentially important energy loss to the system in addition to possibly damaging the laser. A number of experimental[1-7] and theoretical[8-11] studies of laser backscatter indicate that an appreciable amount of energy is reflected back from the target with a modified spectrum. In this Letter we describe experiments which include both time-integrated and time-resolved energy and spectral measurements, and compare these results with stimulated-Brillouin-backscattering predictions.

The experimental setup used in these studies consists of a neodymium:glass laser beam ($\lambda_0 = 1.064$ μm) focused with either an $f/14$ or an $f/1.9$ lens onto a slab target in an evacuated chamber.[4] The pulse duration used is either 900, 250, or 50 psec full width at half-maximum energy with energy ≤ 100 J. A prepulse identical in shape to the main pulse with approximately 5% of the pulse energy is usually applied 700 psec ahead of the main pulse. For the main pulse the irradiance at the focal spot is in the range $I \leq 5 \times 10^{15}$ W/cm^2. Calorimeters independently monitor the incident energy and the energy reflected back through the lens.

A semiquantitative measurement of the angular distribution of the scattered 1.06-μm laser light at solid angles *other than back through the focusing lens* was performed.[12] By rotating the target, we determine that the intensity of this scattered radiation peaks at the specular-reflection angle from the target, has an angular extent of about $\pm 40°$, and has a total energy content of 5–10% of the incident laser energy. The specularly reflected energy per solid angle is typically small compared to the direct backscattered energy. However, the total energies scattered outside and inside the solid angle subtended by the $f/14$ lens ($\pm 2°$) are comparable. The fact that we independently detect specular reflection allows us to conclude that the much more intense light which is directly backscattered through the lens is the result of some anomalous process. Henceforth we will discuss only the 1.06-μm radiation backscattered through the lens solid angle.

It was verified that the backscattered light is